

Integrated Analysis of Cytoskeleton-Associated lncRNAs and Their Regulatory Networks in Mouse Oocyte Maturation

Lin Luping^{1a,b,c}, Suresh V Chinni^{2b, d*} and Genliang Li^{3c}

Abstract: With the increase in maternal age and the impact of environmental stress, the decline in ovarian reserve and oocyte quality has emerged as a primary cause of infertility. Dysfunction of cytoskeletal proteins plays a central role in this process. This study aims to examine the differential expression and regulatory functions of cytoskeleton-associated long non-coding RNAs (lncRNAs) during the development of mouse oocytes at the germinal vesicle (GV) and metaphase II (MII) stages. This study employed bioinformatics analyses and machine learning techniques to analyze publicly accessible data from the Gene Expression Omnibus (GEO) database, which comprised 13 samples of Germinal Vesicle (GV) stage oocytes and 15 samples of Metaphase II (MII) stage oocytes. Differential expression analysis, weighted gene co-expression network analysis (WGCNA), and interaction network construction were performed to screen for lncRNAs closely related to oocyte development. A total of 338 differentially expressed lncRNAs (DE-lncRNAs) with statistical significance were identified, including 136 upregulated and 202 downregulated lncRNAs, indicating their potential roles in the transition from the GV to the MII stage during oocyte development. WGCNA further identified modules strongly correlated with cytoskeletal proteins by integrating these results with the differentially expressed lncRNAs. A total of 47 candidate lncRNAs were shortlisted. Subsequently, LASSO regression and random forest algorithms were applied to identify six key lncRNAs from the candidate set. Combined with miRNA prediction and target gene analysis, a lncRNA-miRNA-mRNA regulatory network was constructed, revealing that these key lncRNAs may indirectly regulate downstream target gene expression through specific miRNAs. Furthermore, Gene Ontology (GO) and Kyoto Encyclopedia of Genes and Genomes (KEGG) enrichment analyses indicated that these key lncRNAs are primarily involved in cytoskeletal remodeling, cell proliferation, and differentiation, and may play critical roles in follicle structure formation and oocyte development. This study systematically mapped the regulatory network of lncRNAs during oocyte development and elucidated the lncRNA-miRNA-mRNA interactions. The results emphasize the key roles of lncRNAs in cytoskeletal remodeling and oocyte maturation, providing valuable insights for the diagnosis and treatment of ovarian disorders.

Keywords: Cytoskeletal proteins, long non-coding RNAs, mouse oocyte development, ceRNA, reproductive health

1. Introduction

In modern society, the postponement of childbearing age and the increasing impact of environmental stressors have presented women with challenges such as diminished ovarian reserve and reduced oocyte quality, which have become major contributing factors to infertility (Hart, 2016; Barragán et al., 2017). Moreover, the rising prevalence of malignancies in young women has made fertility preservation for cancer patients a pressing concern (Rodriguez-Wallberg et al., 2021). These challenges highlight the need for improved understanding of the molecular mechanisms

governing oocyte development, as they are directly related to reproductive health and fertility outcomes. Understanding the molecular regulatory mechanisms of oogenesis holds significant scientific and clinical importance for improving reproductive health and advancing assisted reproductive technologies (ART).

The cytoskeleton is essential to maintaining the structure and function of oocytes throughout maturation. Composed mainly of microtubules, actin filaments, and intermediate filaments, it participates in key biological processes during oocyte maturation, including spindle assembly, chromosome segregation, and cytoplasmic reorganization (Roeles & Tsiavalariis, 2019). Microtubules are critical for spindle formation and chromosome segregation in oocytes. For example, p21-activated kinase 4 (PAK4) is a serine/threonine kinase vital for regulating microtubule stability (Wu et al., 2022). Inhibition of PAK4 in murine oocytes results in destabilization of microtubules, which subsequently causes defective spindle assembly and erroneous chromosome segregation (He et al., 2019). RAB35 GTPase also regulates microtubule stability in mouse oocytes; its deficiency results in spindle formation defects and asymmetric division failures (Y. Zhang et al., 2019).

Actin filaments are essential for polar body extrusion and spindle migration during oocyte maturation. The interaction

Authors information:

^aDepartment of Obstetrics and Gynaecology, Affiliated Hospital of Youjiang Medical University for Nationalities, Baise, Guangxi, 533300, CHINA. E-mail: linluping1989@163.com¹

^bDepartment of Biochemistry, Faculty of Medicine, Bioscience and Nursing, MAHSA University, Jenjarom 42610, Selangor MALAYSIA. E-mail: linluping1989@163.com¹, venkatasuresh@mahsa.edu.my²

^cYoujiang Medical University for Nationalities School of Basic Medical Sciences, Baise, Guangxi, CHINA. E-mail: linluping1989@163.com¹, ligenliang@ymun.edu.cn³

^dDepartment of Periodontics, Saveetha Dental College and Hospitals, Saveetha Institute of Medical and Technical Sciences, Chennai 602105, INDIA. E-mail: cvsureshgupta@gmail.com²

*Corresponding Author: cvsureshgupta@gmail.com

Received: May 11, 2025

Accepted: July 17, 2025

Published: December 12, 2025

between actin filaments and microtubules, which involves specific molecular mechanisms such as the coordinated action of motor proteins and the regulation of filament dynamics, ensures correct spindle positioning and successful polar body extrusion. In human oocytes, this interaction is fundamental for spindle assembly and accurate chromosome segregation (Roeles & Tsiavaliaris, 2019). Moreover, the organization of the actin network can influence microtubule behavior, affecting the overall oocyte maturation process (Colin et al., 2018). In summary, the dynamic remodeling and coordination of the cytoskeleton are indispensable for oocyte maturation. Any disruption to these structures may lead to oocyte maturation abnormalities.

Although the importance of the cytoskeleton in oocyte maturation is well-established, the regulatory mechanisms of its dynamic remodeling remain incompletely elucidated. In recent years, the discovery of non-coding RNAs (ncRNAs) has provided new insights. Long non-coding RNAs (lncRNAs) can act as competing endogenous RNAs (ceRNAs) by binding to miRNAs, regulating the expression of protein-coding genes (Salmena et al., 2011; Mattick et al., 2023). Accumulating evidence shows that lncRNAs are involved in various reproductive processes, including primordial germ cell development and migration (Jiao et al., 2018), oocyte maturation, and ovarian cell apoptosis and proliferation (L. Zhang et al., 2023). For example, the lncRNA PWNR2 functions as a ceRNA, inhibiting the interaction between miR-92b-3p and its target mRNA TMEM120B, and thus plays a crucial role in oocyte maturation (Wei et al., 2022). Additionally, studies have revealed significant differences in lncRNA profiles between MII oocytes and granulosa cells (GCs), with higher lncRNA expression in GCs compared to MII oocytes (Ernst et al., 2018).

lncRNAs can also influence gene expression by interacting with chromatin. They can act as scaffolds or guides for chromatin-modifying complexes, targeting specific genomic loci and modulating their epigenetic states (Mangiavacchi et al., 2023). During oogenesis, lncRNAs may regulate the expression of cytoskeleton-related genes through these mechanisms, contributing to cytoskeletal remodeling.

However, the molecular mechanisms by which lncRNAs in cytoskeletal remodeling through the lncRNA-miRNA-mRNA regulatory network remain largely unexplored. This study seeks to elucidate the role of the lncRNA-miRNA-mRNA regulatory axis in the dynamic remodeling of the cytoskeleton during oogenesis. We specifically hypothesize that lncRNAs, through their interactions with miRNAs and mRNAs, are pivotal in regulating cytoskeletal remodeling during oocyte maturation. By identifying novel competing endogenous RNA (ceRNA) regulatory pathways associated with oocyte development, this research aims to establish a theoretical foundation for the development of innovative therapeutic strategies to enhance oocyte quality and fertility outcomes, thereby contributing to the reduction of reproductive disease incidence.

2. Materials and methods

2.1 Data Collection and Preprocessing

All datasets used in this study were publicly available and downloaded from the Gene Expression Omnibus (GEO) database (<https://www.ncbi.nlm.nih.gov/geo/>). We searched the database for species limited to *Mus musculus*. The GSE137458 dataset was selected due to its provision of lncRNA expression data from both Germinal Vesicle (GV) stage oocytes (prophase I-arrested immature state with intact nuclear envelope) and Metaphase II (MII) stage oocytes (metaphase II-arrested mature state after polar body extrusion), which are directly pertinent to our research focus on the developmental transition from the GV to the MII stage. The GSE141190 dataset was selected because of its extensive data on mouse oocyte development, offering additional valuable information for a comprehensive analysis. From GSE141190, we selected seven raw GV-stage oocyte samples (GSM4196729 to GSM4196735) and eight MII-stage oocyte samples (GSM4196770 to GSM4196777) as control samples to complement the data from GSE137458, increasing the sample size and potentially improving the reliability of our analysis.

The lncRNA expression profiles of mouse oocytes at the germinal vesicle (GV) stage were retrieved and downloaded using the "GEOquery" package in R. The two datasets were merged. To correct for batch effects caused by non-biological technical variations, the ComBat function from the "sva" R package was applied (Leek et al., 2012). ComBat utilizes an empirical Bayes framework to adjust gene expression data by estimating and removing batch-specific effects, ensuring that observed differences in expression reflect biological variation rather than technical inconsistencies. Before merging, we carefully examined the data formats of the two datasets. Both had gene expression values in a tabular format, but the column headers and some metadata labels differed slightly. We standardized the column headers to ensure consistency. Regarding the data, GSE137458 had a relatively smaller number of samples compared to GSE141190. To address this, we did not perform any data subsampling but instead weighted the contribution of each dataset during the batch correction process to avoid overemphasizing the larger dataset. After batch correction, principal component analysis (PCA) was performed to assess its effectiveness. As a result, we obtained a new integrated dataset comprising 13 GV-stage and 15 MII-stage oocyte samples, which was used for all subsequent analyses. This study adhered to the data access policies of each database utilized.

A total of 102 human cytoskeleton-related genes were obtained from the GeneCards database. These genes were mapped to their mouse homologs through homology mapping, resulting in 98 mouse cytoskeleton-related genes, which were subsequently used for downstream analyses.

We also conducted a data quality assessment of the public database data. For the GSE137458 and GSE141190 datasets, the missing value proportion was below 5%, which was acceptable. The sample quality control metrics, such as RNA integrity number (RIN), were available for most samples and indicated that the RNA quality was relatively high, with an average RIN value above 7.0, ensuring the reliability of the gene expression data.

2.2 Screening and Analysis of Differentially Expressed lncRNAs

To identify lncRNAs most closely associated with cytoskeletal proteins, the GTF annotation file provided by the R package AnnoProbe (version 0.1.6) was used to differentiate between mRNAs and lncRNAs. Expression matrices for mRNAs and lncRNAs were separately extracted for further analyses.

Differential expression analysis of the lncRNA expression matrix was conducted using the limma package (version 3.50.0) (Ritchie et al., 2015). The comparison was made between the MII-stage group (n = 15) and the GV-stage group (n = 13). Differentially expressed lncRNAs (DElncRNAs) were identified based on the following criteria: $|\log_2\text{Fold Change}| > 0.25$, $p\text{-value} < 0.05$.

The identified DElncRNAs were then used for subsequent analysis. Hierarchical clustering analysis was performed using the pheatmap package in R. Euclidean distance and hierarchical clustering methods were applied to produce heatmaps and visualize expression patterns. In the heatmap, the color scale represents the relative expression levels of lncRNAs. Red indicates high expression, and blue indicates low expression. This color scheme is clearly defined to assist readers in interpreting the expression patterns of different lncRNAs.

2.3 Weighted Gene Co-expression Network Analysis (WGCNA) and Identification of Significant Modules

The WGCNA package (version 1.70-3) in R was employed to construct a weighted gene co-expression network using the WGCNA algorithm (Langfelder & Horvath, 2008). Pearson correlation coefficients were calculated to evaluate the similarity among gene expression profiles. These correlations were then raised to a power function to achieve an approximate scale-free topology in the network.

We used the PickSoftThreshold function to determine the optimal soft-thresholding power (β). After testing various β values, we found that when $\beta = 3$, the average connectivity approached zero, and the scale-free topology fit index exceeded 0.85 (Figure 2A). This indicated that the constructed network conformed to the properties of a scale-free network. We chose this parameter because it provided the best balance between network stability and the ability to detect meaningful gene modules. Other values of β led to a network that was too sparse or too dense, making it difficult to interpret the co-expression relationships accurately.

Gene modules are clusters of densely interconnected genes within the co-expression network. WGCNA applies hierarchical clustering to identify gene modules, which are color-coded for visualization. The dynamic tree cut approach was utilized to detect distinct gene modules. During module detection, the adjacency matrix (which measures topological similarity) was converted into a topological overlap matrix (TOM), followed by hierarchical clustering to identify gene modules.

To explore the relationship between gene modules and cytoskeletal proteins, Pearson correlation analysis was performed between the module eigengenes (MEs)—which represent the first principal component of each module, reflecting the overall expression pattern—and the expression of cytoskeletal protein-

related genes. Modules that showed significant correlations with cytoskeletal proteins were identified as key modules.

The structure of the co-expression modules was visualized through heatmaps of gene network topological overlap. Furthermore, a hierarchical clustering dendrogram of module eigengenes, along with the corresponding heatmap, was used to summarize the associations among the identified modules.

Finally, cytoskeletal protein-related differentially expressed lncRNAs (cytoskeletal protein-related DElncRNAs) were identified by taking the intersection between DElncRNAs and the lncRNAs present in the cytoskeletal protein-related modules.

It should be noted that the WGCNA algorithm has several limitations. It is sensitive to data noise, and outliers in the gene expression dataset can potentially affect module identification. We pre-processed the data to mitigate this by removing genes with extremely low expression levels. We performed multiple rounds of analysis with different data subsets to ensure the identified modules' consistency.

2.4 Identification of Hub lncRNAs Using LASSO Regression and Random Forest Analysis

To compute and select linear models while retaining valuable variables, the LASSO (Least Absolute Shrinkage and Selection Operator) regression was performed using the glmnet package in R. A binomial distribution was applied for LASSO classification, and the model was established by choosing the lambda value corresponding to the minimum cross-validated error. This approach resulted in a model with optimal performance and included 10-fold cross-validation to ensure reliability.

Subsequently, random forest (RF) analysis was conducted using the RandomForest function in R. Ultimately, the ntree parameter was set to 1000, and the computation of the proximity matrix was activated (proximity = TRUE). According to the importance measures, namely, Mean Decrease Accuracy (MDA) and Mean Decrease Gini (MDG), the top 30 cytoskeleton-related DElncRNAs were identified as key genes selected by the random forest algorithm.

By integrating the results from both the LASSO regression and random forest analysis, the most significant feature lncRNAs were identified and selected as hub lncRNAs in this study.

LASSO regression and random forest analysis may face challenges when dealing with high-dimensional data, such as overfitting. To address this, we performed feature selection prior to applying these algorithms to reduce the dimensionality of the data. Additionally, we used cross-validation techniques to optimize the model parameters and evaluate the performance of the models.

2.5 lncRNA-miRNA-mRNA Regulatory Network Analysis

In this study, six hub lncRNAs were selected for further analysis. To predict their potential interacting miRNAs, four established bioinformatics tools were employed: Miranda, PITA, TargetScan, and RNAhybrid. Each of these tools has its own algorithmic principle. Miranda uses a seed-based pairing algorithm to predict miRNA-target interactions, which is sensitive

to the sequence complementarity in the miRNA seed region. PITA predicts miRNA-target binding based on the free energy change of the miRNA-mRNA duplex formation, considering the local RNA secondary structure. TargetScan focuses on conserved miRNA-binding sites in the 3'-UTR of mRNAs, and RNAhybrid predicts hybridization between miRNA and mRNA by calculating the minimum free energy of the duplex. Each tool has its own advantages and limitations. Miranda can identify many potential targets but may have a relatively high false-positive rate. PITA's consideration of RNA secondary structure makes its predictions more biologically relevant, but it may miss some targets due to the complexity of structure prediction. TargetScan's reliance on conserved binding sites may lead to omission of non-conserved but functional targets, and RNAhybrid's accuracy may be affected by the precision of the energy calculation model.

We integrated the prediction results from all four algorithms to identify candidate miRNAs. Only the intersecting miRNAs were retained to improve the reliability and specificity of the predictions.

Subsequently, to further investigate the downstream regulatory networks of these candidate miRNAs, five widely recognized algorithms were used to predict their potential target mRNAs. These included TargetScan, Miranda, miRmap, PITA, and PicTar. The intersection of these prediction results was taken to identify a set of high-confidence target genes, ensuring reliability and minimizing false-positive results in the subsequent construction of the lncRNA-miRNA-mRNA regulatory network.

We compared the prediction results of different tools. For example, TargetScan and Miranda often predicted overlapping targets, but there were differences as well. TargetScan was more likely to identify conserved targets, while Miranda could detect some non-conserved ones. The differences were mainly due to their different algorithmic principles and data sources. By taking the intersection of multiple predictions, we aimed to obtain a more reliable set of candidate molecules.

2.6 GO and KEGG Pathway Enrichment Analysis

Gene Ontology (GO) analysis is a commonly used method for large-scale functional enrichment investigations, encompassing three main categories: Biological Process (BP), Molecular Function (MF), and Cellular Component (CC). In this study, the target genes of cytoskeleton-related differentially expressed lncRNAs were subjected to GO and Kyoto Encyclopedia of Genes and Genomes (KEGG) pathway enrichment analysis using the ClueGO plugin in Cytoscape software (Bindea et al., 2009).

For the GO and KEGG enrichment analysis results, when terms such as "cytoskeleton organization" and "MAPK signaling pathway" were significantly enriched, we further examined their relationships with oocyte development and cytoskeletal remodeling.

2.7 Ethical Statement

This study did not involve human subjects or animal experiments. All experimental data were obtained from publicly available databases (Gene Expression Omnibus, GEO), specifically datasets GSE137458 and GSE141190. The use of these datasets

complies with the access policies and terms of use of the GEO database and has been authorized by the relevant institutions. Throughout the research process, strict adherence to data privacy and ethical guidelines was maintained to ensure the lawful use and analysis of the data.

2.8 Statistical Analysis

All statistical analyses in this study were conducted using R software (version 4.1.2). Spearman's correlation test was employed to evaluate the association between two variables. The Wilcoxon rank-sum test was applied to compare differences between two groups, while the Kruskal-Wallis test was used to compare three or more groups. A two-sided p-value of less than 0.05 was considered statistically significant.

3. Results

3.1 Differentially Expressed lncRNAs Related to Oocyte Development

By comparing the lncRNA expression profiles between the GV group and the MII control group, a total of 338 significantly differentially expressed lncRNAs (DELncRNAs) were detected ($p < 0.05$, $|\text{Log}_2\text{FC}| > 0.25$), as shown in Figure 1A. Among these, 136 lncRNAs were upregulated, and 202 lncRNAs were downregulated. The heatmap in Figure 1B further displays the top 10 lncRNAs with the most significant differential expression. In the volcano plot (Figure 1A), the x-axis depicts the \log_2 fold change in lncRNA expression between the MII-stage and GV-stage groups, while the y-axis shows the $-\log_{10}$ of the p-value. Data points above the horizontal dashed line (representing a p-value threshold of 0.05) and beyond the vertical dashed lines (representing a \log_2 fold change threshold of ± 0.25) are considered differentially expressed lncRNAs. The distribution of these points illustrates the overall pattern of differential expression, with some lncRNAs being notably upregulated and others downregulated. In the heatmap (Figure 1B), each row corresponds to an lncRNA, and each column represents a sample. The color gradient from blue to red indicates a gradual rise in expression levels, allowing for a visual comparison of lncRNA expression patterns across different samples.

3.2 Construction of Weighted Gene Co-expression Network and Identification of Cytoskeleton-Related Modules

In this study, the WGCNA method was applied to analyze lncRNAs related to cytoskeletal proteins. The results of the scale-free topology and mean connectivity analysis showed that when the soft-thresholding power (β) was set to 3, the average connectivity approached zero, and the scale-free topology fit index exceeded 0.85 (Figure 2A), indicating that the constructed network conformed to the properties of a scale-free network. A total of eight co-expression modules were identified using WGCNA. lncRNAs that did not cluster into any of the modules

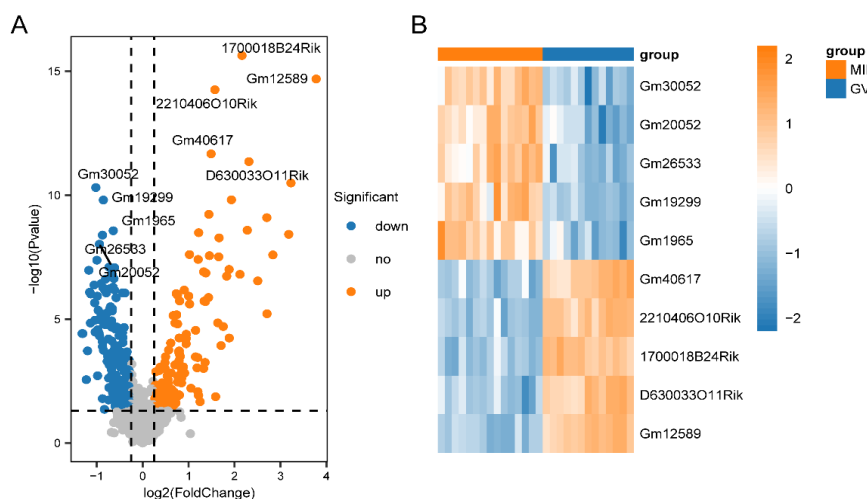


Figure 1. Identification of Differentially Expressed lncRNAs (DElncRNAs) During Oocyte Development. (A) Volcano plot illustrating the distribution of DElncRNAs between the GV group and the MII control group (B) Heatmap showing the top-ranked DElncRNAs with the most significant differential expression

were assigned to the grey module, which was excluded from further analysis (Figure 2B).

To explore the relationships between modules and assess their association with cytoskeletal proteins, correlation analyses were conducted between the module eigengenes (MEs), and the results were visualized as a heatmap to illustrate the network of module relationships (Figure 2C). By correlating the MEs of the eight modules with cytoskeleton-related genes, the blue module, comprising 264 lncRNAs, was found to show the strongest positive correlation with cytoskeletal proteins ($r = 0.8401$, $P < 0.05$), as indicated in the module-trait relationship heatmap (Figure 2D). Given its statistical significance, subsequent analyses primarily focused on the blue module, which most likely represents the regulatory roles associated with cytoskeletal proteins.

Furthermore, an intersection analysis was performed between the differentially expressed lncRNAs (DElncRNAs) and the lncRNAs within the cytoskeleton-related module, resulting in the identification of 47 lncRNAs closely linked with cytoskeletal proteins (Figure 2E). Wilcoxon rank-sum tests further confirmed that these lncRNAs exhibited statistically significant expression differences between the GV and MII groups ($p < 0.05$, Figure 2F). In the module-trait relationship heatmap (Figure 2D), each cell represents the correlation coefficient between a module eigengene and cytoskeleton-related genes, with the p-value shown in parentheses below. The color legend clearly indicates the strength and direction of the correlations, with red representing positive correlations and blue representing negative correlations. This format allows readers to easily identify the modules most strongly associated with cytoskeletal proteins.

3.3 Identification of Key lncRNAs Using Two Machine Learning Algorithms

To further identify key cytoskeleton-related lncRNAs, this study applied two machine learning algorithms: LASSO regression

and random forest analysis. Through LASSO regression analysis, six key lncRNAs were ultimately identified (Figure 3A-B). In the random forest analysis, the top 30 cytoskeleton-related lncRNAs with significant feature importance were selected based on two evaluation metrics: Mean Decrease Accuracy (MDA) and Mean Decrease Gini (MDG) (Figure 3C-D). By integrating the results from both methods and taking the intersection, a total of six key cytoskeleton-related lncRNAs were finally determined as hub lncRNAs for subsequent analyses. These six lncRNAs are: BC023719, 1700026F02Rik, 4930567H12Rik, Gm20319, Gm46355, and 6430573P05Rik (Figure 3E). In the LASSO regression coefficient profiles (Figure 3A), the horizontal axis represents the logarithm of the lambda parameter, and the vertical axis shows the coefficients of the independent variables. As the lambda value changes, the coefficients of the lncRNAs are shrunk towards zero. The point where the coefficients stabilize and the cross-validation error is minimized (Figure 3B) indicates the optimal set of lncRNAs selected by the LASSO regression. In the random forest analysis, the error rate plotted against the number of classification trees (Figure 3C) shows how the model's performance improves as more trees are added. The top 30 lncRNAs ranked by MDA and MDG (Figure 3D) represent the most influential features in the model, and the intersection with the LASSO-selected lncRNAs (Figure 3E) yields the final set of hub lncRNAs.

3.4 Validation of Hub lncRNAs

Further validation of the expression patterns of the identified hub lncRNAs was performed using a heatmap. The results show that all hub lncRNAs exhibited low expression levels at the GV stage, which increased progressively during oocyte development (Figure 4).

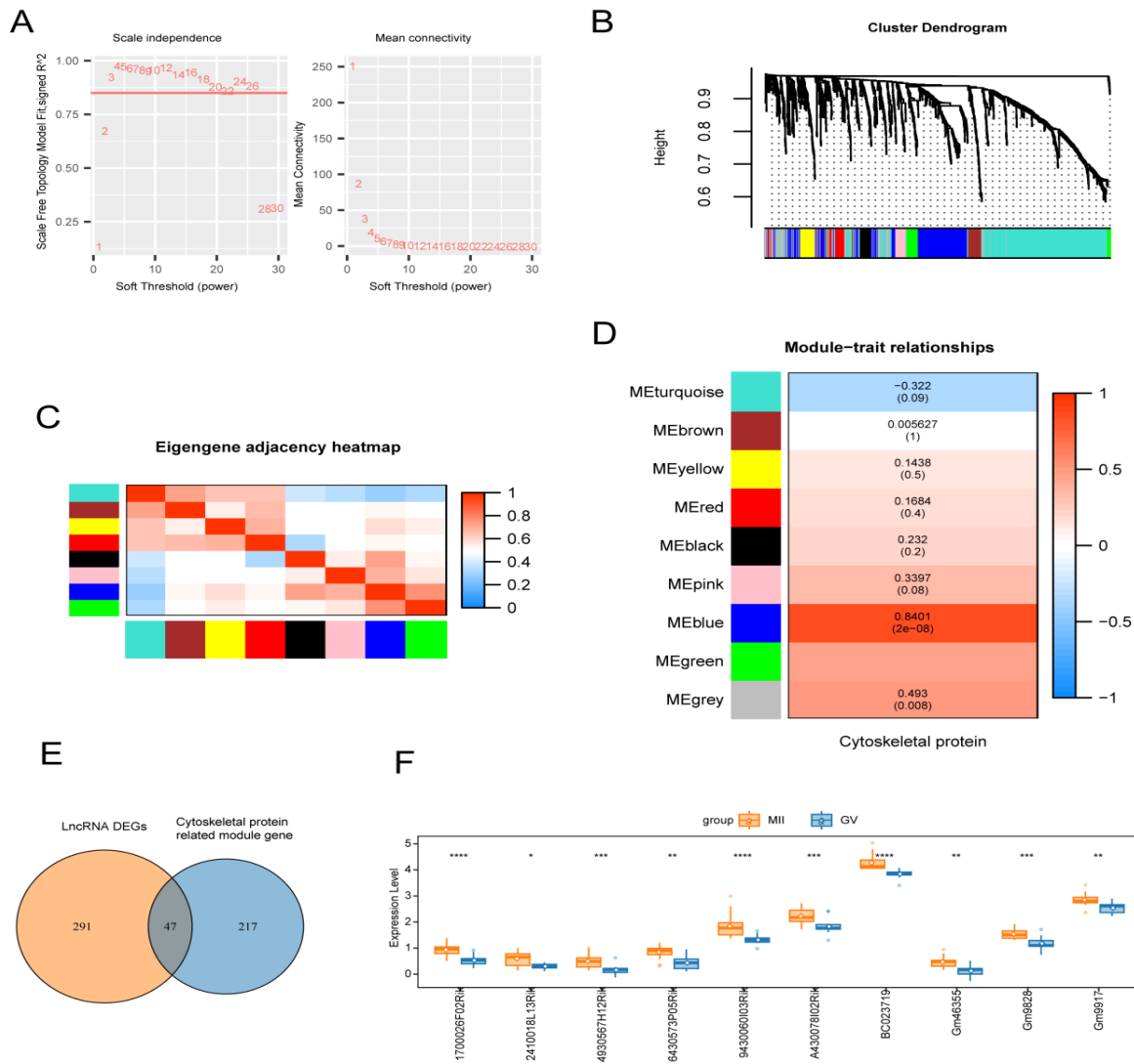


Figure 2. Construction of the WGCNA Co-expression Network

(A) Scale-free topology model fit index (R^2) when the soft-thresholding power $\beta = 3$. The high R^2 value above 0.85 indicates that the constructed weighted gene co-expression network adheres to the scale-free property, which is crucial for analyzing gene-gene relationships in a biological context. (B) Identification of distinct co-expression modules from the lncRNA expression network in the GV stage. A different color represents each module. The clustering of lncRNAs into modules based on their co-expression patterns helps in understanding the coordinated functions of these non-coding RNAs during oocyte development. This visual representation provides insights into the similarities and differences in the expression trends of different modules. (C) Relationships among the identified modules. Top: Hierarchical clustering dendrogram of module eigengenes (MEs), summarizing the clustering of modules. Branches of the dendrogram (meta-modules) group positively correlated module eigengenes. Bottom: Heatmap showing the correlations between module eigengenes. Each row and column represent an eigengene of a module (color-coded). In the heatmap, red indicates high adjacency, and blue indicates low adjacency. Red squares along the diagonal correspond to meta-modules. (D) Heatmap showing the correlations between consensus module eigengenes and cytoskeleton-related genes. Each row corresponds to a consensus module, and each column corresponds to a trait (cytoskeletal proteins). The numbers represent correlation coefficients, with p-values shown in parentheses below. The color legend indicates the strength and direction of the correlations. The strong positive correlation of the blue module with cytoskeletal proteins ($r = 0.8401$, $P < 0.05$) suggests its significant role in cytoskeletal regulation during oocyte development. (E) Venn diagram illustrating the intersection between differentially expressed lncRNAs (DELncRNAs) and lncRNAs within the blue module. The identification of 47 lncRNAs at this intersection implies that these lncRNAs are likely to be involved in both the differential expression events between GV and MII stages and the regulation of cytoskeletal proteins. (F) Box plots showing the expression differences of the top 10 lncRNAs between GV and MII control groups. Statistical significance was assessed by the Wilcoxon rank-sum test. Asterisks indicate p-values: **** $p < 0.0001$, *** $p < 0.001$, ** $p < 0.01$, * $p < 0.05$. The significant differences in expression levels of these lncRNAs further support their potential importance in oocyte development.

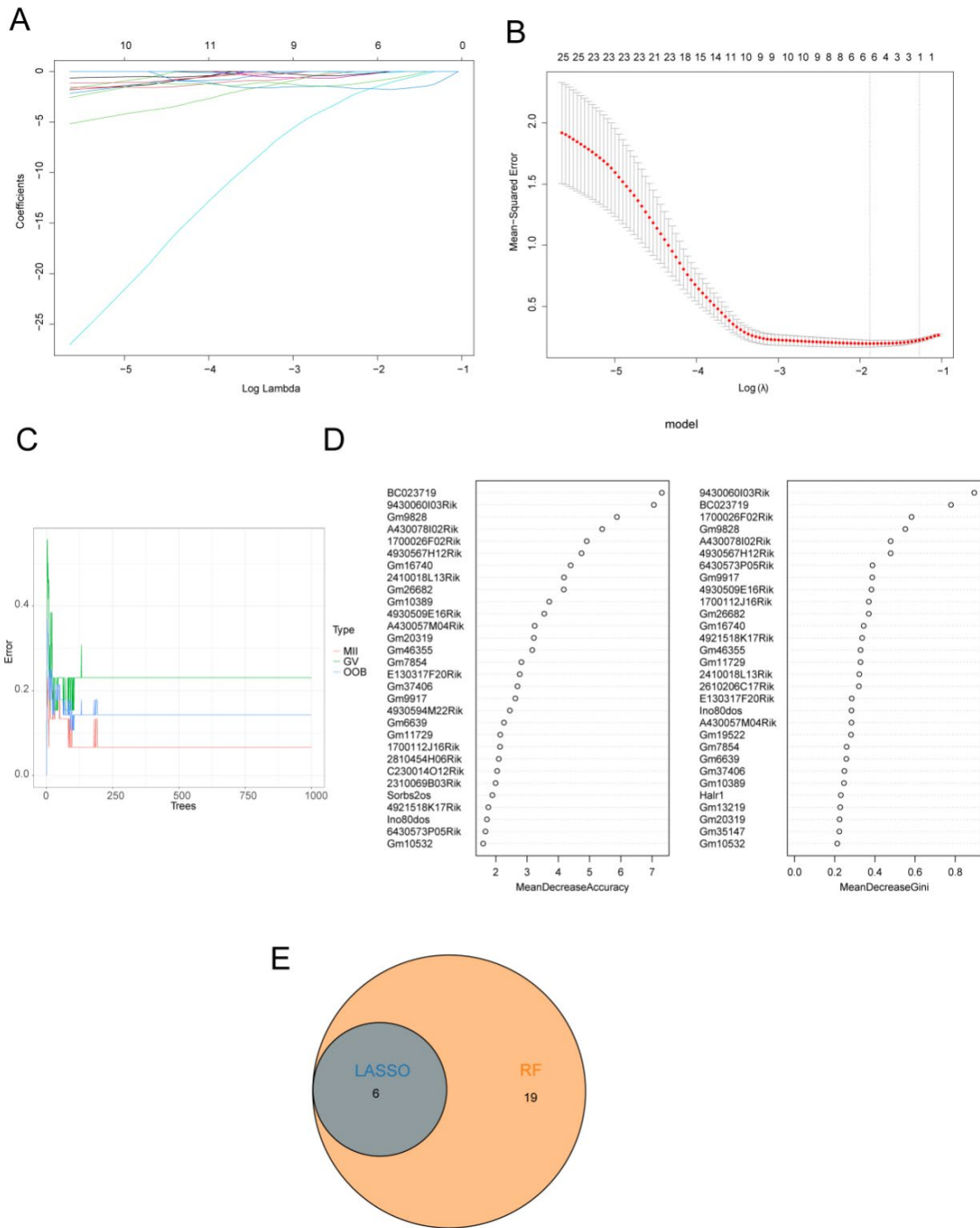


Figure 3. Selection of Candidate Diagnostic Biomarkers for Oocyte Development Progression Using Machine Learning Approaches

Note: (A) LASSO regression coefficient profiles of the candidate variables. The horizontal axis represents the logarithm of the lambda parameter, and the vertical axis represents the coefficients of the independent variables. As the lambda value changes, the coefficients of the candidate IncRNAs are shrunk, and the most relevant IncRNAs are retained in the model. (B) The cross-validation curve for the LASSO regression model shows the confidence intervals for each lambda value. The optimal lambda value is selected based on the minimum cross-validation error, ensuring the model's reliability and generalization ability. (C) Random forest model error rates plotted against the number of classification trees, highlighting the key IncRNAs identified. As the number of trees increases, the error rate stabilizes, and the importance of different IncRNAs can be evaluated based on metrics like MDA and MDG. (D) The top 30 cytoskeleton-related differentially expressed IncRNAs (DEIncRNAs) ranked by two importance measures in the random forest analysis: Mean Decrease Accuracy (MDA) and Mean Decrease Gini (MDG). These rankings help identify the most influential IncRNAs in the context of cytoskeletal regulation during oocyte development. (E) Venn diagram illustrating the intersection of IncRNAs identified by machine learning algorithms (LASSO regression and random forest). The six IncRNAs at the intersection are considered the most significant and are selected as hub IncRNAs for further in-depth analysis.

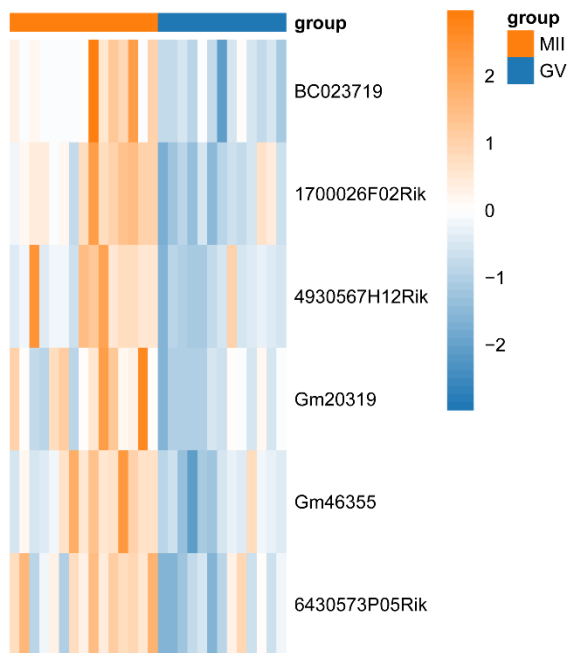


Figure 4. Heatmap Showing the Expression Levels of Hub lncRNAs in GV and MII Stages. The heatmap clearly shows the differential expression of the six hub lncRNAs between the GV and MII stages. The upward trend in expression from GV to MII stages indicates their potential involvement in the regulatory processes associated with oocyte maturation.

We also generated box plots to demonstrate the distribution of hub lncRNA expression levels in various sample groups. The box plots illustrate the median, interquartile range, and any outliers in the data, providing a more comprehensive view of the expression variability.

3.5 Analysis of the lncRNA-miRNA-mRNA Regulatory Axis

To further demonstrate the regulatory mechanisms of the key lncRNAs, this study focused on the six most critical cytoskeleton-related lncRNAs and predicted their potential interacting miRNAs. Using four bioinformatics tools for miRNA prediction, 370 candidate miRNAs potentially interacting with the six lncRNAs were identified by taking the intersection of the results (Figure 5A). To explore the downstream regulatory roles of these miRNAs, five additional prediction tools were applied to identify their target mRNAs. By intersecting the prediction results, 608 potential target genes were obtained (Figure 5B). These findings suggest that the main lncRNAs may form lncRNA-miRNA-mRNA regulatory axes by interacting with specific miRNAs, thereby indirectly regulating gene expression in ovarian development.

We constructed a more detailed lncRNA-miRNA-mRNA regulatory network diagram. In this diagram, each lncRNA is represented as a circular node, miRNAs as triangular nodes, and mRNAs as rectangular nodes. The edges connecting the nodes represent the predicted interactions, with arrows indicating the direction of regulation. The thickness of the edges can be adjusted to represent the confidence level of the prediction, based on the number of algorithms that predicted the interaction. This diagram

offers a more intuitive understanding of the complex regulatory relationships.

3.6 Key Regulatory Roles of the lncRNA-miRNA-mRNA Axis in Follicular Development and Its Biological Processes

To further elucidate the regulatory mechanisms of key lncRNAs in follicular development, this study constructed lncRNA-miRNA-mRNA regulatory axes and conducted an in-depth functional analysis of the target genes of the associated miRNAs (Figure 6). GO functional enrichment analysis revealed that the miRNA target genes play essential roles in multiple key biological processes during follicular development, particularly in cell proliferation, differentiation, signal transduction, and cytoskeletal dynamics remodeling. Among the enriched pathways, terms such as "positive regulation of developmental process," "positive regulation of cell differentiation," and "positive regulation of cell population proliferation" emphasized the potential involvement of these miRNA target genes in promoting the rapid proliferation and differentiation of follicular cells.

For example, in the context of cell proliferation, the target genes may regulate the cell cycle by interacting with key cell-cycle-related proteins. In cell differentiation, they may modulate the expression of transcription factors that are crucial for determining the fate of follicular cells. Regarding cytoskeletal dynamics remodeling, the target genes might influence the polymerization and depolymerization of actin filaments and microtubules, which are essential for maintaining the structural stability of follicular cells and facilitating their movement.

In addition, reproductive system-related pathways, such as "reproductive system development" and "reproductive structure development," further suggest that these miRNA target genes may play important roles in ovarian development and functional maturation. Moreover, signaling pathways, including the Wnt signaling pathway and the regulation of the MAPK cascade, revealed a complex interaction between cytoskeletal dynamics and intracellular signal transduction. These pathways are likely to be crucial for coordinating the communication between oocytes and granulosa cells, ensuring synchronized follicular development and intercellular interaction within the follicular microenvironment. Importantly, the organization and dynamic regulation of the cytoskeleton are indispensable across various stages of follicular development. The enrichment of pathways such as "cytoskeleton organization," "actin cytoskeleton organization," and "regulation of cytoskeleton organization" indicates that the miRNA target genes may regulate cytoskeletal remodeling. These processes are vital for maintaining follicular structural stability, establishing oocyte polarity, and ensuring accurate chromosome segregation. Beyond providing mechanical support, the cytoskeleton may also coordinate with signaling networks to influence the proliferation, differentiation, and functional coordination of cells within the developing follicle.

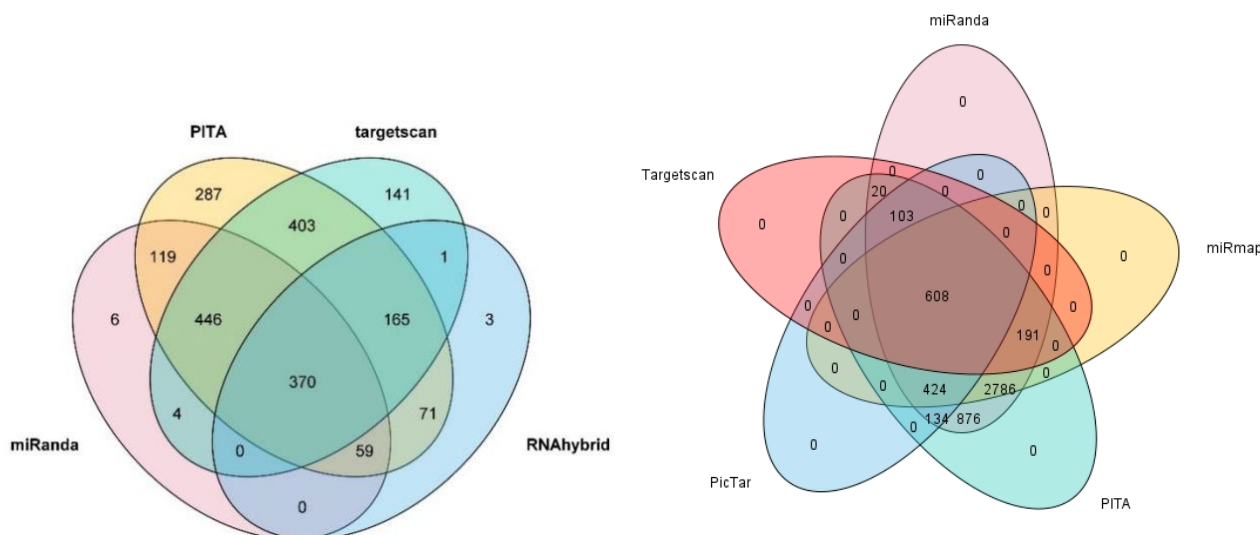


Figure 5. Identification of High-Confidence lncRNA-miRNA Interactions and Identification of miRNA Target Genes

Note: (A) The interaction between lncRNA and miRNA was predicted using four bioinformatics tools (Miranda, PITA, TargetScan, and RNAhybrid). By integrating the predictions from these four tools, 370 candidate miRNAs were identified, which are more likely to interact with six key lncRNAs. (B) The downstream target genes of the 370 candidate miRNAs were predicted using five bioinformatics tools (TargetScan, Miranda, miRmap, PITA, and PicTar). By analyzing the intersection of the results from these tools, 608 potential target genes were identified.

3.7 Signaling Pathways and Cytoskeletal Dynamics Regulated by the lncRNA-miRNA-mRNA Axis During Follicular Development

To further elucidate the mechanisms by which the lncRNA-miRNA-mRNA regulatory axis influences follicular development, KEGG pathway enrichment analysis was conducted to investigate its potential biological functions. The results demonstrated that the miRNA target genes were significantly enriched in several key signaling pathways, including the MAPK, PI3K-Akt, Notch, and Hippo signaling pathways. These pathways are likely involved in granulosa cell proliferation and differentiation, oocyte maturation, cell-cell communication, and the regulation of follicular reserve.

For instance, in the MAPK signaling pathway, activation can lead to the phosphorylation of various downstream targets, which in turn regulate processes such as cell proliferation and differentiation in granulosa cells. In the PI3K-Akt signaling pathway, activation promotes cell survival and growth, which is crucial for the development and maintenance of follicles. The Notch signaling pathway plays a role in cell fate determination and cell-cell communication between granulosa cells and oocytes. The Hippo signaling pathway regulates organ size and tissue homeostasis, which may be relevant to follicular growth and maturation.

In addition, the enrichment of Focal adhesion and Tight junction signaling pathways suggests that granulosa cells may preserve follicular structural integrity through interactions with the extracellular matrix (ECM). The enrichment of VEGF and Chemokine signaling pathways indicates potential roles in angiogenesis and local microenvironment regulation, which are essential for follicular growth and immune balance.

Notably, the significant enrichment of the Regulation of Actin Cytoskeleton signaling pathway underscores the critical role of cytoskeletal dynamics during follicular development. By providing essential mechanical support, cytoskeletal remodeling may contribute to sustaining oocyte maturation as well as the structural and functional stability of the follicle.

4. Discussion

In this study, the construction of a lncRNA-miRNA-mRNA regulatory axis, combined with several analytical approaches, systematically clarified the functions of key lncRNAs in mouse follicular development, particularly their roles in cytoskeletal dynamic remodeling and the regulation of signaling pathways. Through an integrated analysis involving differential expression analysis, weighted gene co-expression network analysis (WGCNA), LASSO regression, and random forest algorithms, we identified core lncRNAs associated with cytoskeletal regulation and further examined their potential regulatory mechanisms.

Firstly, we employed WGCNA to investigate the co-expression relationships between differentially expressed lncRNAs and cytoskeleton-related genes. In recent years, WGCNA has been widely used in biological research for mining co-expression patterns from high-dimensional gene expression data to identify key regulatory modules and candidate genes (B. Zhang & Horvath, 2005). In our study, WGCNA identified eight co-expression modules, among which the blue module showed the strongest positive correlation with cytoskeleton-related genes ($R > 0.8$, $P < 0.01$). This method's reliability and biological relevance have been

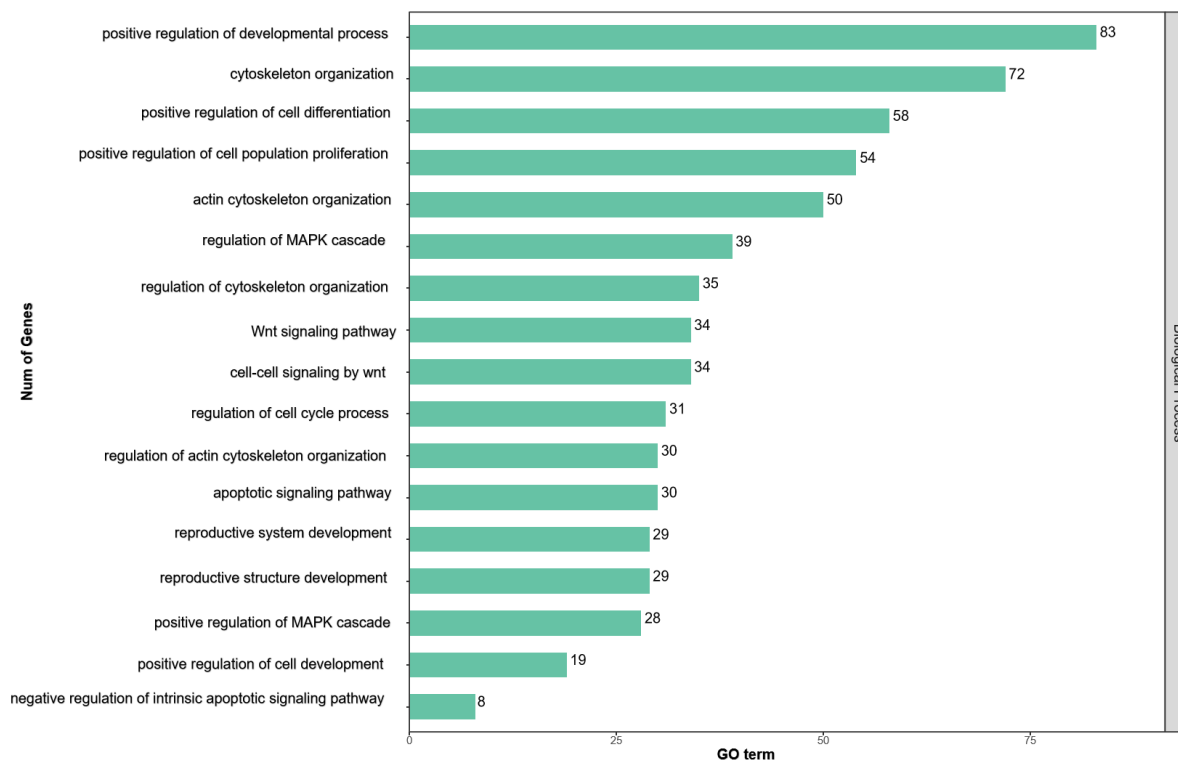


Figure 6. Biological Process Regulation of the LncRNA-miRNA-mRNA Regulatory Axis in Follicular Development.

Note: The figure visually represents the various biological processes in which the lncRNA - miRNA - mRNA regulatory axis is involved during follicular development. The enrichment of these processes in the miRNA target genes indicates the significance of this regulatory axis in orchestrating follicular growth and maturation. The figure depicts the key signaling pathways in which the miRNA target genes are enriched. These pathways are intricately linked to the processes of follicular development, and the lncRNA - miRNA - mRNA regulatory axis appears to play a central role in modulating these pathways.

validated in other models, including identifying key lncRNAs in cancer and cardiovascular diseases (Yin et al., 2020; Song et al., 2023). By intersecting the differentially expressed lncRNAs (DELncRNAs) with those in the blue module, we identified 47 cytoskeleton-related DELncRNAs, which are likely to play essential roles in oocyte polarity establishment, cytoskeletal remodeling, and cytokinesis.

To further pinpoint the most functionally significant lncRNAs, we applied LASSO regression and random forest methods. Through these two machine learning techniques, we ultimately identified six hub lncRNAs, including BC023719, Gm20319, and 1700026F02Rik, which are likely to play dominant roles in regulating follicular development and were subjected to further regulatory network analysis.

Gene Ontology (GO) enrichment analysis revealed that the lncRNA-miRNA-mRNA regulatory axis was significantly enriched in biological processes such as "cytoskeleton organization", "actin cytoskeleton organization", and "regulation of cytoskeleton organization", emphasizing the central role of the cytoskeleton in follicular development. Cytoskeletal dynamic remodeling is necessary for oocyte polarity establishment and meiotic division, particularly in chromosome segregation, maintenance of oocyte morphology, and granulosa cell migration (Mao et al., 2014; Roeles & Tsiavaliaris, 2019). Additionally, GO analysis highlighted

the role of the cytoskeleton in cell proliferation and differentiation, as shown by pathways such as "positive regulation of cell differentiation" and "positive regulation of developmental process", indicating that dynamic cytoskeletal changes regulate cell morphology and interactions, enabling the transition of follicles from the primary stage to the dominant follicle stage (Irlles et al., 2016; Mogollón García et al., 2024).

KEGG pathway enrichment analysis further revealed several classical signaling pathways involved in cytoskeletal regulation and follicular development. Notably, pathways such as "Regulation of Actin Cytoskeleton", "Focal Adhesion", and "PI3K-Akt Signaling Pathway" demonstrated that cytoskeletal dynamics not only provide mechanical stability for granulosa cells but also coordinate cell migration, polarity, and proliferation through integrated signal transduction, thereby establishing the foundation for follicular development (Gardel et al., 2010; Greig & Bulgakova, 2020). Moreover, the MAPK signaling pathway regulated cell adhesion and intercellular communication between granulosa cells, ensuring the organized and coordinated development of follicular cells (Long et al., 2021; Shen et al., 2023). Of particular note, the enrichment of the VEGF signaling pathway suggests that cytoskeletal regulation may contribute to follicular angiogenesis, ensuring an adequate supply of nutrients and energy to the oocyte (Ortega Serrano et al., 2016; Guzmán et al., 2023). The complex interplay between these signaling

pathways and the cytoskeleton highlights the dual role of the cytoskeleton as both a structural scaffold and a key center for signal transduction and developmental regulation during

key lncRNAs could potentially serve as novel diagnostic biomarkers. By quantifying the expression levels of these lncRNAs in ovarian tissue or biological fluids such as follicular fluid, it may

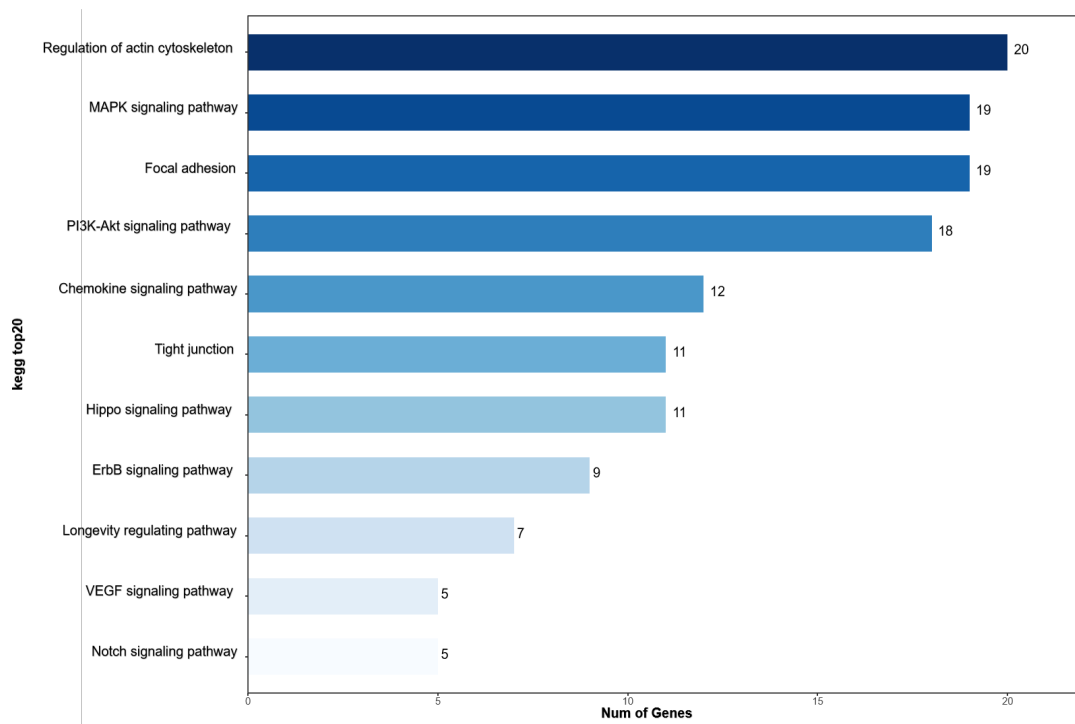


Figure 7. Signaling Pathway Regulation Mediated by the lncRNA-miRNA-mRNA Regulatory Axis During Follicular Development

follicular growth. By constructing the lncRNA-miRNA-mRNA regulatory axis, this study further clarified the mechanisms by which the cytoskeleton is regulated during follicular development. Core lncRNAs may regulate the dynamic remodeling of the cytoskeleton indirectly by modulating downstream miRNAs and mRNAs. For example, the Notch and Hippo signaling pathways play essential roles in the interaction between granulosa cells and oocytes by stabilizing the cytoskeleton and controlling its associated functions (Hu et al., 2019; Hubbard et al., 2019). Similarly, the Focal Adhesion and Tight Junction pathways preserve follicular structural integrity by controlling granulosa cell adhesion and intercellular connections (Yamada et al., 2013; Campbell et al., 2017). These regulatory processes collectively ensure the coordinated organization and functionality of the cytoskeleton during follicular development.

However, it is important to recognize the limitations of this study. The predictions of miRNA-target interactions and the constructed regulatory network are derived from bioinformatics algorithms, which may present certain levels of false-positive and false-negative rates. The data employed in this study were obtained from public databases. Although we performed quality assessments, the sample size remained relatively limited, which may influence the generalizability of the results. Additionally, the biological roles of the identified lncRNAs require further verification through experimental investigations.

In the context of ovarian disease diagnosis and treatment, our findings have relevant implications. For example, the identified

key lncRNAs could potentially serve as novel diagnostic biomarkers. By quantifying the expression levels of these lncRNAs in ovarian tissue or biological fluids such as follicular fluid, it may be possible to evaluate the quality of oocytes and the health of the ovarian follicles. This could provide valuable information for early detection of ovarian disorders related to oocyte maturation defects, such as polycystic ovary syndrome (PCOS) and premature ovarian insufficiency (POI) (D. Li et al., 2021; Y. Li & Tan, 2021).

Furthermore, targeting these lncRNAs or components of the lncRNA-miRNA-mRNA regulatory network might represent a promising therapeutic approach. For instance, if a specific lncRNA is demonstrated to play a critical role in promoting abnormal cytoskeletal remodeling in diseased ovaries, developing small molecule inhibitors or RNA-based therapies to modulate its expression could potentially restore normal oocyte development and improve fertility outcomes. However, before translating these findings into clinical practice, further pre-clinical and clinical studies are necessary to validate the efficacy and safety of such interventions.

To progress toward clinical application, future research should emphasize the experimental validation of these findings, particularly through in vivo studies examining the functional roles of the six identified hub lncRNAs. Overexpression and knockdown experiments should be conducted to evaluate how these lncRNAs regulate cytoskeletal dynamics and affect oocyte development. By manipulating the expression of these lncRNAs in mouse models, we can explore their direct effects on spindle formation, chromosome segregation, and overall oocyte maturation. Additionally, assessing how these lncRNAs interact with their target miRNAs and mRNAs in vivo will provide essential insights

into their mechanistic roles during oogenesis. These experimental validations are crucial for confirming the clinical relevance of these lncRNAs and their potential as therapeutic targets in reproductive medicine.

This study identifies key lncRNAs significantly associated with cytoskeletal regulation during oocyte development, particularly between the GV and MII phases. Through various computational methods, including WGCNA, LASSO regression, and random forest analysis, we identified six hub lncRNAs—BC023719, Gm20319, 1700026F02Rik, 4930567H12Rik, Gm46355, and 6430573P05Rik—that play central roles in regulating cytoskeletal dynamics. Gene ontology and KEGG pathway enrichment analyses further support the involvement of these lncRNAs in important pathways such as "cytoskeleton organization," "MAPK signaling," and "PI3K-Akt signaling." Additionally, the construction of a lncRNA-miRNA-mRNA regulatory network suggests that these lncRNAs may indirectly affect follicular development by modulating downstream miRNA and mRNA targets.

5. Acknowledgements

The authors sincerely thank the National Center for Biotechnology Information (NCBI) and the Gene Expression Omnibus (GEO) database for providing the publicly available datasets (GSE137458 and GSE141190) used in this study. We also express our gratitude to the GeneCards database for supplying crucial information on cytoskeleton-related genes, which was essential for our analysis.

We acknowledge the financial support provided by the MAHSA Research Grant RP193-10/22.

Special thanks go to our mentors for their invaluable guidance and continuous support throughout this research. Their expertise and dedication have been instrumental in the completion of this study.

Finally, the authors are grateful to the reviewers and editors for their constructive comments, which have significantly enhanced the quality of this manuscript.

6. References

- Barragán, M., Pons, J., Ferrer-Vaquer, A., Cornet-Bartolomé, D., Schweitzer, A., Hubbard, J., Auer, H., Rodolose, A., & Vassena, R. (2017). The transcriptome of human oocytes is related to age and ovarian reserve. *Molecular Human Reproduction*, 23(8), 535–548.
- Bindea, G., Mlecnik, B., Hackl, H., Charoentong, P., Tosolini, M., Kirilovsky, A., Fridman, W.-H., Pagès, F., Trajanoski, Z., & Galon, J. (2009). ClueGO: A cytoscape plug-in to decipher functionally grouped gene ontology and pathway annotation networks. *Bioinformatics (Oxford, England)*, 25(8), 1091–1093.
- Campbell, H. K., Maiers, J. L., & DeMali, K. A. (2017). Interplay between tight junctions & adherens junctions. *Experimental Cell Research*, 358(1), 39–44.
- Colin, A., Singaravelu, P., Théry, M., Blanchoin, L., & Gueroui, Z. (2018). Actin-network architecture regulates microtubule dynamics. *Current Biology : CB*, 28(16), 2647–2656.e4.
- Ernst, E. H., Nielsen, J., Ipsen, M. B., Villesen, P., & Lykke-Hartmann, K. (2018). Transcriptome analysis of long non-coding RNAs and genes encoding paraspeckle proteins during human ovarian follicle development. *Frontiers in Cell and Developmental Biology*, 6, 78.
- Gardel, M. L., Schneider, I. C., Aratyn-Schaus, Y., & Waterman, C. M. (2010). Mechanical integration of actin and adhesion dynamics in cell migration. *Annual Review of Cell and Developmental Biology*, 26, 315–333.
- Greig, J., & Bulgakova, N. A. (2020). Interplay between actomyosin and E-cadherin dynamics regulates cell shape in the drosophila embryonic epidermis. *Journal of Cell Science*, 133(15), jcs242321.
- Guzmán, A., Hernández-Coronado, C. G., Gutiérrez, C. G., & Rosales-Torres, A. M. (2023). The vascular endothelial growth factor (VEGF) system as a key regulator of ovarian follicle angiogenesis and growth. *Molecular Reproduction and Development*, 90(4), 201–217.
- Hart, R. J. (2016). Physiological Aspects of Female Fertility: Role of the Environment, Modern Lifestyle, and Genetics. *Physiological Reviews*, 96(3), 873–909.
- He, Y.-T., Yang, L.-L., Luo, S.-M., Shen, W., Yin, S., & Sun, Q.-Y. (2019). PAK4 regulates actin and microtubule dynamics during meiotic maturation in mouse oocyte. *International Journal of Biological Sciences*, 15(11), 2408–2418.
- Hu, L.-L., Su, T., Luo, R.-C., Zheng, Y.-H., Huang, J., Zhong, Z.-S., Nie, J., & Zheng, L.-P. (2019). Hippo pathway functions as a downstream effector of AKT signaling to regulate the activation of primordial follicles in mice. *Journal of Cellular Physiology*, 234(2), 1578–1587.
- Hubbard, N., Prasasya, R. D., & Mayo, K. E. (2019). Activation of notch signaling by oocytes and Jag1 in mouse ovarian granulosa cells. *Endocrinology*, 160(12), 2863–2876.
- Irls, P., Elshaer, N., & Piulachs, M.-D. (2016). The notch pathway regulates both the proliferation and differentiation of follicular cells in the panoistic ovary of *blattella germanica*. *Open Biology*, 6(1), 150197.
- Jiao, J., Shi, B., Wang, T., Fang, Y., Cao, T., Zhou, Y., Wang, X., & Li, D. (2018). Characterization of long non-coding RNA and messenger RNA profiles in follicular fluid from mature and immature ovarian follicles of healthy women and women with polycystic ovary syndrome. *Human Reproduction (Oxford, England)*, 33(9), 1735–1748.
- Langfelder, P., & Horvath, S. (2008). WGCNA: An R package for weighted correlation network analysis. *BMC Bioinformatics*, 9, 559.
- Leek, J. T., Johnson, W. E., Parker, H. S., Jaffe, A. E., & Storey, J. D. (2012). The sva package for removing batch effects and other

- unwanted variation in high-throughput experiments. *Bioinformatics (Oxford, England)*, 28(6), 882–883.
- Li, D., Wang, X., Dang, Y., Zhang, X., Zhao, S., Lu, G., Chan, W.-Y., Leung, P. C. K., & Qin, Y. (2021). lncRNA GCAT1 is involved in premature ovarian insufficiency by regulating p27 translation in GCs via competitive binding to PTBP1. *Molecular Therapy - Nucleic Acids*, 23, 132–141.
- Li, Y., & Tan, Y. (2021). Bioinformatics analysis of ceRNA network related to polycystic ovarian syndrome. *Computational and Mathematical Methods in Medicine*, 2021, 9988347.
- Long, H., Yu, W., Yu, S., Yin, M., Wu, L., Chen, Q., Cai, R., Suo, L., Wang, L., Lyu, Q., & Kuang, Y. (2021). Progesterone affects clinic oocyte yields by coordinating with follicle stimulating hormone via PI3K/AKT and MAPK pathways. *Journal of Advanced Research*, 33, 189–199.
- Mangiavacchi, A., Morelli, G., & Orlando, V. (2023). Behind the scenes: How RNA orchestrates the epigenetic regulation of gene expression. *Frontiers in Cell and Developmental Biology*, 11, 1123975.
- Mao, L., Lou, H., Lou, Y., Wang, N., & Jin, F. (2014). Behaviour of cytoplasmic organelles and cytoskeleton during oocyte maturation. *Reproductive Biomedicine Online*, 28(3), 284–299.
- Mattick, J.S., Amaral, P.P., Carninci, P. *et al.* (2023). Long non-coding RNAs: Definitions, functions, challenges and recommendations. *Nature Reviews. Molecular Cell Biology*, 24(6), 430–447.
- Mogollón García, H. D., de Andrade Ferrazza, R., Ochoa, J. C., de Athayde, F. F., Vidigal, P. M. P., Wiltbank, M., Kastelic, J. P., Sartori, R., & Ferreira, J. C. P. (2024). Landscape transcriptomic analysis of bovine follicular cells during key phases of ovarian follicular development. *Biological Research*, 57(1), 76.
- Ortega Serrano, P. V., Guzmán, A., Hernández-Coronado, C. G., Castillo-Juárez, H., & Rosales-Torres, A. M. (2016). Reduction in the mRNA expression of sVEGFR1 and sVEGFR2 is associated with the selection of dominant follicle in cows. *Reproduction in Domestic Animals = Zuchthygiene*, 51(6), 985–991.
- Ritchie, M. E., Phipson, B., Wu, D., Hu, Y., Law, C. W., Shi, W., & Smyth, G. K. (2015). Limma powers differential expression analyses for RNA-sequencing and microarray studies. *Nucleic Acids Research*, 43(7), e47.
- Rodriguez-Wallberg, K. A., Hao, X., Marklund, A., Johansen, G., Borgström, B., & Lundberg, F. E. (2021). Hot Topics on Fertility Preservation for Women and Girls-Current Research, Knowledge Gaps, and Future Possibilities. *Journal of Clinical Medicine*, 10(8).
- Roeles, J., & Tsiavalariis, G. (2019). Actin-microtubule interplay coordinates spindle assembly in human oocytes. *Nature Communications*, 10(1), 4651.
- Salmena, L., Poliseno, L., Tay, Y., Kats, L., & Pandolfi, P. P. (2011). A ceRNA hypothesis: The rosetta stone of a hidden RNA language? *Cell*, 146(3), 353–358.
- Shen, M., Li, T., Feng, Y., Wu, P., Serrano, B. R., Barcenas, A. R., Qu, L., & Zhao, W. (2023). Effects of quercetin on granulosa cells from prehierarchical follicles by modulating MAPK signaling pathway in chicken. *Poultry Science*, 102(7), 102736.
- Song, G.-Y., Guo, X.-N., Yao, J., Lu, Z.-N., Xie, J.-H., Wu, F., He, J., Fu, Z.-L., & Han, J. (2023). Differential expression profiles and functional analysis of long non-coding RNAs in calcific aortic valve disease. *BMC Cardiovascular Disorders*, 23(1), 326.
- Wei, L., Xia, H., Liang, Z., Yu, H., Liang, Z., Yang, X., & Li, Y. (2022). Disrupted expression of long non-coding RNAs in the human oocyte: The possible epigenetic culprits leading to recurrent oocyte maturation arrest. *Journal of Assisted Reproduction and Genetics*, 39(10), 2215–2225.
- Wu, T., Dong, J., Fu, J., Kuang, Y., Chen, B., Gu, H., Luo, Y., Gu, R., Zhang, M., Li, W., Dong, X., Sun, X., Sang, Q., & Wang, L. (2022). The mechanism of acentrosomal spindle assembly in human oocytes. *Science (New York, N.Y.)*, 378(6621), eabq7361.
- Yamada, T., Kuramitsu, K., Rikitsu, E., Kurita, S., Ikeda, W., & Takai, Y. (2013). Nectin and junctional adhesion molecule are critical cell adhesion molecules for the apico-basal alignment of adherens and tight junctions in epithelial cells. *Genes to Cells : Devoted to Molecular & Cellular Mechanisms*, 18(11), 985–998.
- Yin, X., Wang, P., Yang, T., Li, G., Teng, X., Huang, W., & Yu, H. (2020). Identification of key modules and genes associated with breast cancer prognosis using WGCNA and ceRNA network analysis. *Aging*, 13(2), 2519–2538.
- Zhang, B., & Horvath, S. (2005). A general framework for weighted gene co-expression network analysis. *Statistical Applications in Genetics and Molecular Biology*, 4, Article17.
- Zhang, L., Zou, J., Wang, Z., & Li, L. (2023). A subpathway and target gene cluster-based approach uncovers lncRNAs associated with human primordial follicle activation. *International Journal of Molecular Sciences*, 24(13).
- Zhang, Y., Wan, X., Wang, H.-H., Pan, M.-H., Pan, Z.-N., & Sun, S.-C. (2019). RAB35 depletion affects spindle formation and actin-based spindle migration in mouse oocyte meiosis. *Molecular Human Reproduction*, 25(7), 359–372.